Journal of Pharmaceutical and Biomedical Analysis 48 (2008) 876–884

Contents lists available at ScienceDirect

Journal of Pharmaceutical and Biomedical Analysis

journal homepage: www.elsevier.com/locate/jpba

The distribution pattern of intravenous [^{14}C] artesunate in rat tissues by quantitative whole-body autoradiography and tissue dissection techniques

Qigui Li*, Lisa Xie, Jing Zhang, Peter J. Weina

Division of Experimental Therapeutics, Walter Reed Army Institute of Research, Silver Spring, MD, USA

ARTICLE INFO

Article history:
Received 21 March 2008
Received in revised form 1 July 2008
Accepted 2 July 2008
Available online 30 July 2008

Keywords:
[^{14}C] Artesunate
Dihydroartemisinin
QWBA
LSC
Tissue distribution
Pharmacokinetics
Rats

ABSTRACT

Quantitative whole-body autoradiography (QWBA) and liquid scintillation counting (LSC) have been conducted to determine the metabolic profiles and tissue distribution of [^{14}C] labeled artesunate (AS) injection in rats. The QWBA technique showed more accurate results in the quantification of radioactivity in 40 organs and tissues, compared to 19 organs with the LSC technique. The benefit of QWBA was especially apparent on measurements of bile, bone marrow, and gland organs; however, the LSC method produced more relevant findings than QWBA. Particularly, the LSC method allowed access to the following distribution patterns that were unavailable via QWBA performance: such as pharmacokinetic evaluation of radiolabeled AS in blood and plasma, tissue/plasma partition coefficients, conversion pathway of AS to dihydroartemisinin (DHA, an active and major metabolite of AS), unchanged AS and DHA in plasma, mass balance assessment, urinary and faecal eliminations, drug pathway with conjugation, [^{14}C] AS binding with RBC and plasma protein, and metabolites identification. Even though the each method has its own advantages, common profiles were obtained from the two processes as shown in the results of the biliary metabolism, long-lasting metabolites, tissue distribution profiles, and multiple concentration peaks, which indicate a [^{14}C] AS enterohepatic circulation.

1. Introduction

Whole-body autoradiography, in its present form, has been developed from Ullberg's original method [1] and has been further modernized by utilizing image analysis programs for converting the obtained gray scale image into quantitative data [2]. The quantitative analysis of autoradiographs can be obtained with a [^{14}C]-labeled compound by the use of a radiosensor, or image plate (IP). The resultant experiments have shown a linear correlation between relative intensity and radioactivity. The correlation is observed in a wide range between 10 and 50,000 dpm orders of radioactivity. Furthermore, the IP is capable of approximately 100 times greater sensitivity than any X-ray film which has been demonstrated by the use of a [^{14}C] radioactive standard source and by experimentally provided [^{14}C] radioactive spots developed on a TLC plate with macroautoradiographs. Currently, a combination of the IP and BAS2000, a computerized image display system, has been used as the quantitative whole-body autoradiography (QWBA) in the investigation of the tissue distribution, pharmacokinetics (PK), and toxicity of radiolabeled compounds in animals [3–7].

Traditionally, the method for carrying out distribution studies and metabolic profiles is by liquid scintillation counting (LSC) in dissected and homogenized organs and tissues. Unfortunately, measurements after dissection yield quantitative concentration data for only a limited, pre-selected number of organs. On the other hand, QWBA is a quantitative detection method by also using radiolabeled compounds with a very high local resolution which includes all organs and many small substructures. Recently many scientists have sought to establish the improved QWBA, which would replace the LSC method for cutting time and energy costs, and would provide: (i) a detailed picture of the distribution of radioactivity at select dose levels and time points in animals; (ii) images of the time course of radioactivity in blood and select tissues (approximate half-life and AUC); (iii) data on urinary and faecal excretions of radioactivity and an estimate of the proportion of radioactive metabolites; (iv) tissue information on the proportion of parent drug versus metabolites in tissue samples extracted

* Corresponding author at: Department of Pharmacology, Division of Experimental Therapeutics, Walter Reed Army Institute of Research, 503 Robert Grant Avenue, Silver Spring, MD 20307-5100, USA. Tel.: +1 301 319 9351; fax: +1 301 319 7360.
E-mail address: qigui.li@amedd.army.mil (Q. Li).

0731-7085/$ – see front matter © 2008 Elsevier B.V. All rights reserved.
doi:10.1016/j.jpba.2008.07.015

from the whole-body sections; and (v) indications of possible tissue binding [8–10].

However, when using QWBA several factors must be considered in comparison with those obtained by conventional LSC methods. These include differences in capabilities in some distribution aspects, various tissue exposition of drug based on the unbound fraction in plasma, the drug concentration at sites of therapeutic activity and toxicity, the routes of excretion, the self-absorption of radioactivity in various tissues, as well as its transfer across blood–brain barriers. Recently, a tissue distribution evaluation of [^{14}C] artesunate (AS) by using dissection of pre-selected tissues from animals, followed by LSC method has been reported in our laboratory 2 years ago [11].

The present study was therefore designed to address these issues in tissue distribution and metabolic profiles. This study was used to identify the largest sources of section variation and develop a method to minimize these sources of errors with QWBA assay. Tissue homogenate data [11] were used to compare and calibrate radiolabeled AS. Thus, a comparison was made between the accuracy of QWBA and LSC techniques in presenting the distribution patterns following a single intravenous injection 5 mg/kg dose of [^{14}C] AS in male SD rats.

2. Materials and methods

2.1. Chemicals

The test unlabeled compound used in this study is artesunic acid (4-(10′dihydro-artemisinin-oxymethyl) succinate; AS), which was manufactured as a phosphate salt with 0.3 M PBS (pH 8.1) and obtained from the Walter Reed Chemical Inventory System. Unlabeled AS (WR256283, BN: BQ38841, Lot N# 2.03) was purchased from Knoll AG and rebottled by BASF Pharmaceuticals. It was supplied through the Division of Experimental Therapeutics at Walter Reed Army Institute of Research (WRAIR, Silver Spring, MD). The one lot of [16-^{14}C] AS (Lot No. 10839-113) used in this study and was synthesized by Research Triangle Institute (Research Triangle Park, NC). The stated specific activity and radiochemical purity was 17.63 mCi/mmol (45.86 μCi/mg) and 97.0%, respectively. The same unlabeled AS and radiolabeled compounds were used in WRAIR for the LSC study and in Quest Pharmaceutical Services, L.L.C. (QPS, Newark, DE), which is our project contract company, for QWBA evaluation. All other materials used in the study were provided by commercial suppliers and all analytical reagents were of standard laboratory reagent grade.

2.2. Animals

Male Sprague–Dawley rats obtained from Charles River Laboratories were used in these studies of LSC and QWBA. On arrival, the animals were acclimated for 7 days (quarantine) thereby assuring that the rats were 8 weeks of age upon the initiation of dosing. The animals were housed individually in cages maintained in a room with a temperature range of 64–79 F, 34–68% relative humidity, and 12-h light/dark cycles. Food and water were supplied *ad libitum* during quarantine and throughout the study. The animals were fed a standard rodent maintenance diet. Animal protocol was approved by IACUC, WRAIR, and the research was conducted in compliance with the Animal Welfare Act and other federal statutes. Regulations relating to animals and experiments involving animals adhered to the principles stated in the Guide for the Care and Use of Laboratory Animals, NRC Publication, 1996 edition. Pharmaceutical Services, L.L.C. is committed to the highest standards of laboratory animal welfare and is subject to legislation under the Animal Welfare Act (PL 89–544). This study protocol was reviewed and approved by the Institutional Animal Care and Use Committee of QPS (IACUC Protocol Number 004.02).

2.3. Whole-body autoradiography of [^{14}C] AS study

The purpose of this study was to determine the tissue distribution of drug-related material following a single i.v. administration of [^{14}C] AS (5 mg/kg) in male Sprague–Dawley rats using quantitative whole-body autoradiography. This study was not conducted in compliance with the Food and Drug Administration Good Laboratory Practice Regulations and was not inspected by the Quality Assurance Department of QPS. However, it was conducted in the spirit of GLP and good documentation was performed. The procedures described in this protocol were performed in accordance with Quest Pharmaceutical Services, L.L.C. (QPS) standard operating procedures.

On the day of dosing, the [^{14}C] AS intravenous dose solution was prepared at a concentration of 5 mg/ml (138.2 μCi/ml) by dissolving an appropriate quantity of [^{14}C] AS in 0.3 M sodium phosphate buffer solution. The solution was shielded from light and stirred continuously on a magnetic stir plate at room temperature throughout the dosing procedure. A triplicate of pre-dose aliquots (0.025 ml) of [^{14}C] AS dose solution was diluted in 10 ml of ethanol. Aliquots (0.1 ml) of the diluted dose solution were counted for 10 min using liquid scintillation counting to check for the homogeneity and concentration of [^{14}C] AS in the dose solution. The residual dose formulation was stored at approximately −70 °C.

Animals were fasted overnight prior to dosing and then weighed in the morning. Each animal received a single intravenous dose of approximately 5 mg/kg body weight at a dose volume of 1.13 ml/kg via a tail vein, which was determined for each rat based on its individual body weight. After dosing, all rats were returned to their cages. Food was returned to animals approximately 4 h post-dose. Cage side observations of all the rats in the study were performed multiple times during the day of dosing and then at least once daily for the remainder of the study. No obvious abnormalities were observed in animals throughout the course of the study. Next, the rats were deeply anesthetized with 5% isofluorane and frozen by submersion in a bath of hexane cooled to approximately −70 °C with solid carbon dioxide at 0.5, 1, 2, 4, 8, 10, 24, 48, 72, and 96 h after dosing. Carcasses were stored at approximately −20 °C prior to preparation for the whole-body autoradiography.

2.4. Whole-body autoradiography analysis

The frozen carcasses were embedded in 2% carboxymethylcellulose and each block was mounted on the object stage of a cryomicrotome (Leica CM3600 Cryomacrocut, Nussloch, Germany) and maintained at approximately −20 °C. Sagittal, whole-body sections, which were approximately 40 μm thick, were obtained from each carcass, and were supported using adhesive tape (Scotch Tape No. 8210, 3M Ltd., St. Paul, MN, USA). Sections were taken from various levels of each carcass until samples of the following tissues or biological matrices along with QC blood standards were obtained, where possible: Adipose (brown and white), adrenal gland, bile (in bile duct), blood (cardiac), brain (cerebrum, cerebellum), bone, bone marrow, epididymis, esophagus, uveal tract of the eye and lens, Harderian gland, heart, kidney cortex and medulla, large intestine (and contents), liver, lung, lymph node, nasal turbinates, pancreas, pituitary gland, prostate gland, salivary gland, seminal vesicles, skeletal muscle, skin, stomach (and contents), small intestine (and contents), spleen, spinal cord, testis, thymus, thyroid, and urinary bladder (and contents).

Sections were allowed to dry by sublimation in the cryomicrotome at −20 °C for approximately 2 days. Sections were then mounted on cardboard backing and exposed, along with [^{14}C] spiked blood calibration standards, to [^{14}C] sensitive imaging plates (Molecular Dynamics, Sunnyvale, CA, USA). Afterwards, the imaging plates and sections were enclosed in exposure cassettes and exposed in a lead safe at room temperature for 4 days. At the end of the exposure time, the sections were removed from the imaging plate and the plates were then scanned and their images stored onto a QPS computer server using the Typhoon 9410, phosphor image acquisition system (Molecular Dynamics, Sunnyvale, CA, USA).

Quantification, relative to the calibration standards, was performed by image densitometry using MCID image analysis software (Imaging Research, St. Catherine's, Ontario, Canada). Image optical density data was acquired as MDC/mm^2. The autoradiographic standard image data (calibration and internal standards) were then sampled using the MCID software to create a calibrated standard curve and to verify section thickness (40 μm) uniformity. Meanwhile, the actual whole-body sections were used as a reference to identify tissues. Specified tissues, organs, and fluid regions of each image were then analyzed and the tissue concentrations were interpolated from each standard curve in microcuries per gram. Consequentially, tissue concentration data were determined for the tissues and/or contents listed above. Tissue concentrations were then converted, based on the specific activity of the test material, to microgram equivalents per gram of tissue [12–14].

Upper and lower limits of quantitation were also determined and employed for these data. The results and conclusions described are based on digital images that were selected from a complete set of autoradiographs. The clarity observed in the digital images may not be apparent in reproductions obtained by photocopying.

2.5. Pharmacokinetic study

Traditional radioactivity pharmacokinetics (PK) studies involve intermittent blood sampling, estimated by using QWBA, and subsequent determinations of drug concentrations (radioactivity, unchanged AS and DHA) measured in blood and plasma by using the LSC method. The PK evaluation of [^{14}C] AS in the blood of individual rats was conducted with 10 time points by QWBA. Blood radioactivity was then scanned from the rats at 0.5, 1, 2, 4, 8, 10, 24, 48, 72, and 96 h post-dosing when rats were embedded. PK evaluation of [^{14}C] AS in plasma and whole blood was conducted, with 14 time points, by LSC in individual rats. Blood samples (7–8 ml) were then collected from the rats, when euthanized, at 5, 10, and 30 min at 1, 1.5, 3, 6, 12, 24, 48, 72, 96, and 192 h post-dosing. The tissue samples generated from both the QWBA and LSC methods were also reported for PK analysis.

2.6. Liquid scintillation accounting (LSC) studies

Rats treated with single [^{14}C] AS intravenously of groups for tissue dissection were anesthetized at 1, 6, 24, 48, 72, 96, and 192 h, post-dosing. Blood, liver, brain, eyes, adrenals, muscle, lungs, heart, liver, kidneys, spleen, stomach, small intestine, large intestine, perirenal fat and bone marrow samples were removed from each animal by gross dissection. The gastrointestinal tract (GI) was separated into: the stomach (esophagus and stomach), small intestine, and large intestine. Contents were procured from each GI segment and were stored after being flushed with saline. Tissues were rinsed gently, but thoroughly with water to remove remaining traces of blood before storage. Dissecting instruments were also washed between tissue procurements to avoid cross-contamination.

The weighed tissues, contents, faeces, urine, blood, and plasma (approx. 0.2 g) were solubilized with 2 ml of Soluble® tissue solubilizer (PerkinElmer Life and Analytical Sciences, Boston, MA) at 50 °C over night. Total radioactivity in the collected tissue samples was quantified in duplicates. Colored samples were also decolorized by adding a maximum of 0.2 ml of 30% H_2O_2 for 4 h. Scintillation cocktail (Hyonic Fluor; PerkinElmer Boston. MA) solution was then added to the samples and radioactivity was determined in a PerkinElmer Tri-Carb 3100 TR scintillation spectrophotometer (Packard Instrument Co., Downers Grove, IL). Plasma was also analyzed using the HPLC–ECD system to measure the concentration of unchanged AS and dihydroartemisinin (DHA), a main and active metabolite of AS, as described by Li et al. [15].

The procedures followed to obtain freely extractable metabolites and extractable compounds after conjugate splitting are described previously [11]. About 2 ml of plasma and urine, and 1–2 g of faeces were used. Conjugates were then hydrolyzed by glucuronidase (1000 FU/ml) at pH 4.6, 38 °C for 24 h. Active enzymes were checked by phenolphthalein glucuronide at the end of incubation. Urine and faecal samples were incubated for 48 h and fresh enzyme was added after 24 h. Total radioactivity in free, conjugates, and remaining aqueous fractions were measured with liquid scintillation counters. Protein precipitates were dissolved in Soluble® (200 mg in 1 ml) and counted for radioactivity after addition of the scintillation cocktail.

2.7. Data evaluation

For PK, the concentration–time data of [^{14}C] AS in plasma and blood collected during the 192 h treatment period were fitted to a three-compartment open model using a nonlinear, extended least-square fitting procedure (WinNonlin 5.0, Scientific Consulting, Inc. Apex, North Carolina, USA). The area under the curve (AUC) was determined using the linear trapezoidal rule with infinite extrapolation based on the concentration of the last time point divided by the terminal rate constant. Extrapolations to time zero were done using zero concentration for intravenous dosing and using C_0 values determined from the three-compartment model equation at time zero by i.v. route. Mean clearance rate (CL) was determined by dividing the dose by the AUC_{inf} for i.v. injection. Mean residence time (MRT) was determined by dividing the area under the first moment curve (AUMC) by the AUC. The volume of distribution at steady state (V_{ss}) was calculated as the product of CL and MRT. The concentration–time data of unchanged AS and DHA in various tissues were then fitted to a two-compartment open model. The ratio of DHA to AS was calculated by AUC_{DHA}/AUC_{AS}.

The bioequivalence (BE) evaluation of the two methods in blood and various tissues were analyzed by using BE software (WinNonlin 5.0, Pharsight Co., Mountain View, CA, USA) for cross-validation of QWBA and LSC methods. The blood and tissues were considered bioequivalent if the 90% confidence interval (CI) of the mean difference for each variable between QWBA will be within −20% and 25% of the LSC results.

3. Results

3.1. Actual doses received

The actual doses administered to the animals ranged from 4.77 to 5.20 mg/kg in the LSC study and 5.49 to 5.95 mg/kg in the QWBA test. The actual doses received by the LSC rats were approximately 12% higher in QWBA animals; however, it is unlikely that this would affect the cross-validation made in the study.

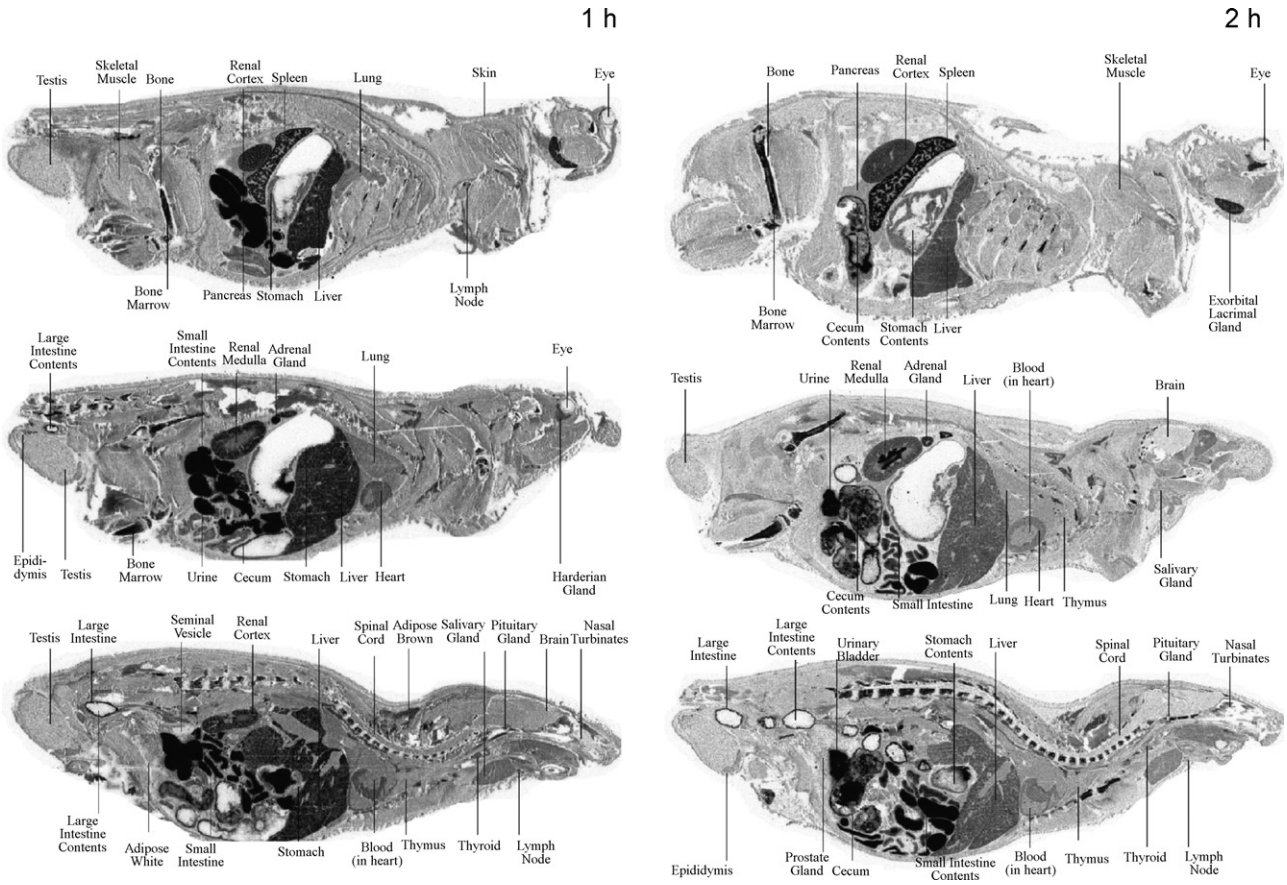

Fig. 1. Photographic autoradiographs representing sections of the left, mid and right regions of the body of male rats sacrificed at 1 h (left), and 2 h (right) following a single intravenous injection of [^{14}C] artesunate (AS) with a radioactivity of 5 mg/138 μCi/kg. 1 h: One hour after single i.v. injection, most of the AS radioactivity was concentrated in the liver and the GI system (small and large intestines, as well as their contents) with light distribution in other tissues. The total amount of [^{14}C] AS in all measured tissues is 972 μg equivalents/rat. 2 h: High density of the radioactivity was still in the GI system, but drug distribution was much less in liver and other tissues when compared to 1 h results. The total radioactivity amount in all measured tissues is 210 μg equivalents that is four times less than that in 1 h animals (n = 2).

3.2. Tissue distribution by QWBA

Patterns of distribution of radioactivity in the tissues of rats at 1, 2, 4, and 96 h following single intravenous administration of [^{14}C] AS at 5 mg/138 μCi/kg are illustrated in Figs. 1 and 2. Mean pharmacokinetic (PK) concentrations of drug-derived radioactivity in blood and other tissues were exhibited in Fig. 3 and Table 1 with 0–96 h sample collections. Concentrations of radioactivity were expressed as the microgram equivalents of AS per gram tissue (μg equivalents/g) with very high concentration in small intestine plus content, spleen, bone marrow and large intestine plus content with long half-lives of 70.9–222.1 h (Table 1). Generally, the higher concentrations and longer half-lives of the radioactivity were found primarily in tissues involved in the distribution and excretion of drug-related material.

The highest concentration of radioactivity in the majority of tissues was observed at 0.5 h post-dose; approximately 84% of radioactivity was amassed in the small intestine and its content while approximately 6% was amassed in the bile (in duct) (Fig. 4). The 90% of total radioactivity present in the small intestine and bile at 0.5 h after i.v. dosing indicated an immediate biliary metabolism of AS in rats. Smaller quantities of radiation (10%) were distributed in other tissues (Fig. 4). Overall, at 0.5 h post-dose, the total amount of radiation in all measured tissues was a 1247 μg equivalent. Furthermore, 1 h after the injection, very high levels of radioactivity were still present in the small intestine and in its contents (83%) while approximately 4.5% of radioactivity was amassed in the urinary bladder and its contents. The total amount of radiation in all measured tissues in 1 h samples was 972 μg equivalents. Two-hour post-dose readings showed that the total radioactivity was significantly reduced to 210 μg equivalents when compared to 1 h data.

Remarkably, 4 h post-dose, drug distribution was significantly increased 2-fold higher to 451 μg equivalents when compared to the two-hour samples in all tissues, and the concentration profiles showed a multiple concentration peaks (Fig. 5, top). This increase in radiation may be related to intestinal re-absorption and the enterohepatic circulation.

Consecutively, radioactivity was rapidly reduced in all tissues, except for the spleen and bone marrow; from 24 to 96 h post-dose (Fig. 4). The total amount of radioactivity in all measured tissues per gram was 72, 42, 31, and 27 μg equivalent at 24, 48, 72, and 96 h, respectively. At 96 h post-dose, the residual activity of 2.8% of total amount collected was still detected in these tissues. During the 96 h experimental period with the QWBA technique, up to 50% of total radioactivity was found in the small and large intestines, their contents and bile (in duct) following the single intravenous injection of [^{14}C] AS (Table 1). Then, the highest levels of total radioactivity were presented following by in the spleen (17.73%), bone marrow (11.88%), kidneys (8.22%), adrenal gland (3.78%), and liver (3.14%), while trace amounts were found in other tissues.

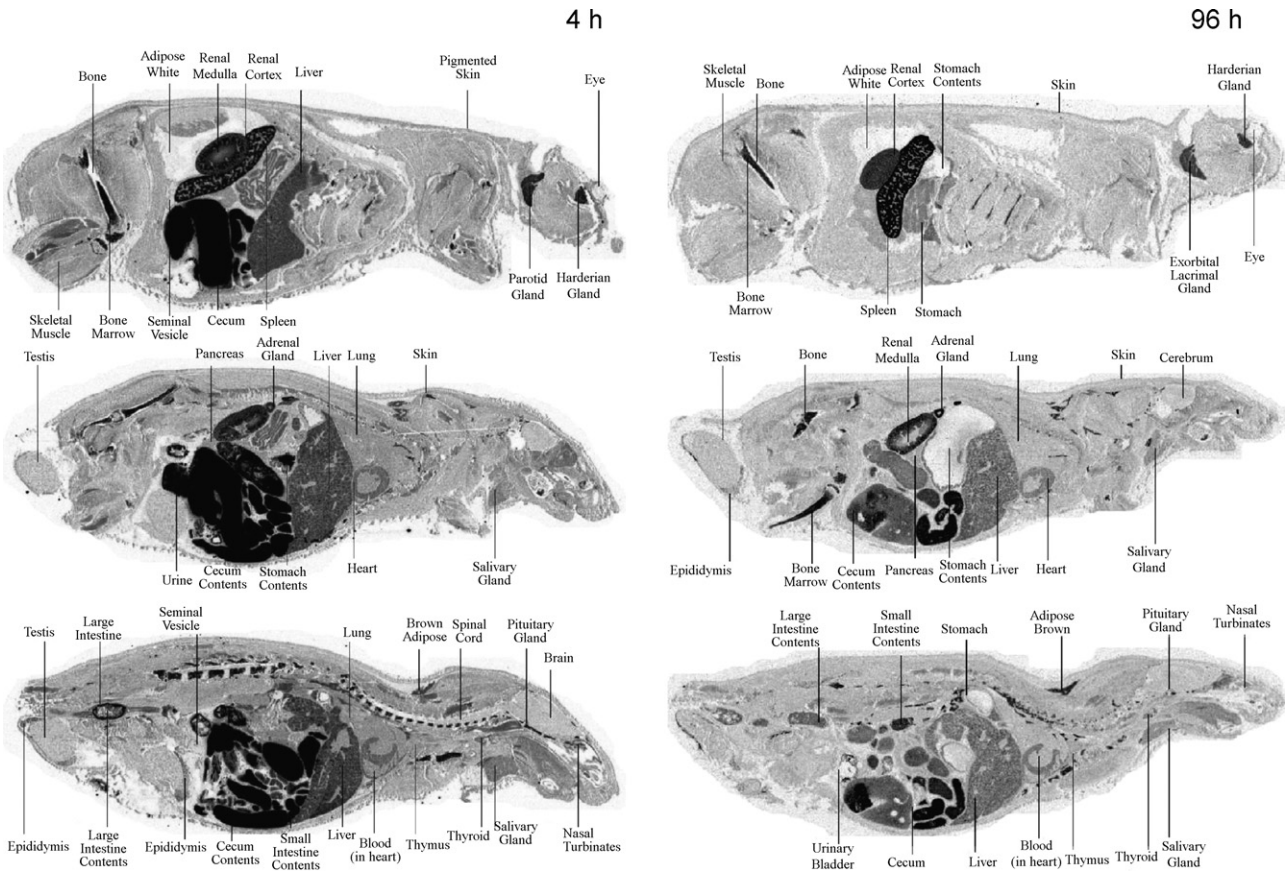

Fig. 2. Photographic autoradiographs representing sections of the left, mid, and right regions of the body of male rats sacrificed at 4 h (left), and 96 h (right) following a single intravenous injection of [^{14}C] artesunate (AS) with a radioactivity of 5 mg/138 μCi/kg. 4 h: Four hours after single i.v. injection, most of the AS radioactivity was concentrated in the GI system with light distribution in other tissues. The total amount of [^{14}C] AS in all measured tissues is 451 μg equivalents, which is two-fold higher than that in 2 h animals. 96 h: Ninety-six hours after injection, the high density of the radioactivity was only found in the spleen, bone marrow, and GI system, but drug distribution was much less in other tissues when compared to 4 h results. The total radioactivity amount in all measured tissues is 27 μg equivalents at 96 h after the treatment (n = 2).

Table 1
Comparison of mean and main tissue PK parameters of [^{14}C] artesunate following a single intravenous injection at 5 mg/20 μCi/kg between by using liquid scintillation counting (LSC) and quantitative whole-body autoradiography (QWBA), as well as an initial establishment on bioequivalence (BE) calculated confidence interval (CI) should fall within a BE limit of −20/25% (90% CI) for the ratio of the product averages

Organs	LSC					QWBA				BE C_{max} and AUC_{96h}
	$t_{1/2}$ (h)	C_{max} (μg/g)	AUC_{96h} (μg · h/g)	% of Total AUC	$K_{t:p}$	$t_{1/2}$ (h)	C_{max} (μg/g)	AUC_{96h} (μg · h/g)	% of Total AUC	
Plasma	76.2	2.63	29.4	0.25	1.00	NA				
Bile (in duct)	NA					111.6	80.17	429.5	3.20	
Blood	98.8	1.74	104.3	1.30	3.51	82.5	2.11	88.9	0.98	Yes
Brain	94.2	1.11	70.7	0.88	2.42	90.5	1.32	61.4	0.68	Yes
Eyes	62.1	1.17	42.5	0.53	1.39	138.9	1.44	93.3	1.04	No
Adrenal gland	109.6	14.17	374.2	4.67	12.69	97.4	13.86	340.1	3.78	Yes
Muscle	105.8	0.74	54.5	0.68	1.84	96.2	0.93	69.7	0.77	Yes
Lungs	123.8	2.11	160.0	2.00	5.40	105.8	2.66	96.9	1.07	No
Heart	108.6	4.19	251.9	3.15	8.53	91.5	3.74	202.5	2.02	Yes
Spleen	154.3	10.16	1860.7	23.24	63.22	222.1	9.12	1595.3	17.73	Yes
Kindeys	94.2	9.01	832.2	10.40	28.25	102.3	7.64	740.2	8.22	Yes
Liver	78.9	6.72	363.3	4.54	12.33	92.6	6.16	293.7	3.14	Yes
Stomach	93.5	1.83	122.1	1.53	4.12	111.3	3.40	137.8	1.53	No
Stomach Content	77.9	2.15	48.7	0.61	1.65	69.6	1.78	50.2	0.55	Yes
Large intestine	69.5	6.54	246.4	3.08	8.35	56.4	5.59	104.6	1.16	Yes
Large intestinal Content	65.6	10.84	862.5	10.77	29.32	76.5	12.21	1055.1	12.83	Yes
Small intestine	74.9	17.08	249.0	3.11	8.43	70.9	15.37	213.2	2.03	Yes
Small intestinal Content	29.4	1106.89	2310.1	28.86	78.49	28.1	1376.92	2745.1	30.51	Yes
Bone marrow	NA					152.9	9.85	1069.4	11.88	
Total amount			8035.33					8996.9[a]		Yes

[a] The actual dose administered to the LSC animals in mean of 5.01 mg/20.73 μCi/kg, and to QWBA rats in mean of 5.63 mg/138 μCi/kg. Therefore, the dose amount in QWBA animals is approximate 12% more than in LSC rats. Mean ± S.D. (n = 3–5). $K_{t:p}$ = tissue/plasma partition coefficients ($AUC_{tissue}/AUC_{plasma}$).

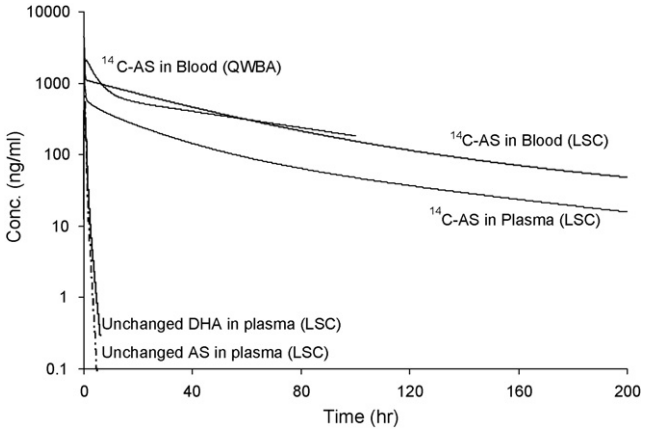

Fig. 3. Total radioactivity (ng equivalents/ml) of [^{14}C] artesunate (AS) in whole blood by QWBA technique (solid-line, 0–96 h) and in blood and plasma by LSC method (dot-line, 0–192 h), as well as unchanged AS and dihydroartemisinin (DHA), an active metabolite of AS, concentration (ng/ml) in plasma by LSC technique (dashed and solid-line) following a single intravenous injection of [^{14}C] AS at 5 mg/138 μCi/kg for QWBA and 5 mg/20 μCi/kg for LSC methods in male rats (n = 2–6).

3.3. Tissue distribution by LSC

Rat tissue samples were collected at 1, 6, 24, 48, 72, 96, and 192 h following single i.v. administration of [^{14}C] AS. Mean radioactivity (μg equivalent/g tissue) in each tissue were measured following single intravenous injection of 5 mg/20 μCi/kg at differing time points. One-hour post-dose approximately 68% of radioactivity in the total measured tissues was amassed in the small intestine and its contents. Smaller quantities of radiation were also distributed in other tissues. The total amount of radiation in all measured tissues per gram was 131 μg equivalents at 1 h after dosing. Six hours post-dose, similar high levels of radioactivity (136 μg equivalents) were still present. Although slowly declining in the intestine and the colon, drug distribution was increased in other tissues of the kidney, spleen, liver, heart, adrenals, blood, muscle, colon and colon content.

From 24 to 96 h, radioactivity rapidly declined in all tissues except for the spleen and kidney (Table 1). The total amount of radioactivity in all measured tissues was 40, 30, 23, 17, and 8 μg equivalent at 24, 48, 72, 96, and 192 h, respectively. At 192 h post-dose the residual radioactivity (close to 2.6% of total amount collected) was still detected in some tissues: the highest concentrations were found in the spleen, kidney, adrenals, and heart. Concentrations of radioactivity in the blood and plasma were still detected 192 h post-dose however the concentration in whole blood was notably higher (2–4-fold) than in plasma. Furthermore, the estimated distribution of [^{14}C] AS in red blood cells (RBC) is approximately 6-fold higher than in plasma. Interestingly, AS was also completely eliminated within 2–3 h (elimination half-life of 0.4 h) indicating that the long-lasting radioactivity was a result of metabolites [11].

Pharmacokinetic parameters calculated from mean levels of total radioactivity, unchanged AS, and unchanged DHA in either whole blood or plasma after single i.v. administration of [^{14}C] AS are shown in Fig. 3. The concentration–time data of [^{14}C] AS in plasma and blood collected during the 192 h of the treatment period were fitted to a three-compartment open model. Radioactivity derived from [^{14}C] AS was eliminated from plasma with half-life of 76.2 h, and from blood with half-life of 98.8 h. Unchanged AS and DHA were eliminated from plasma with half-lives of 0.4 and 0.8 h, respectively. Following the intravenous administration

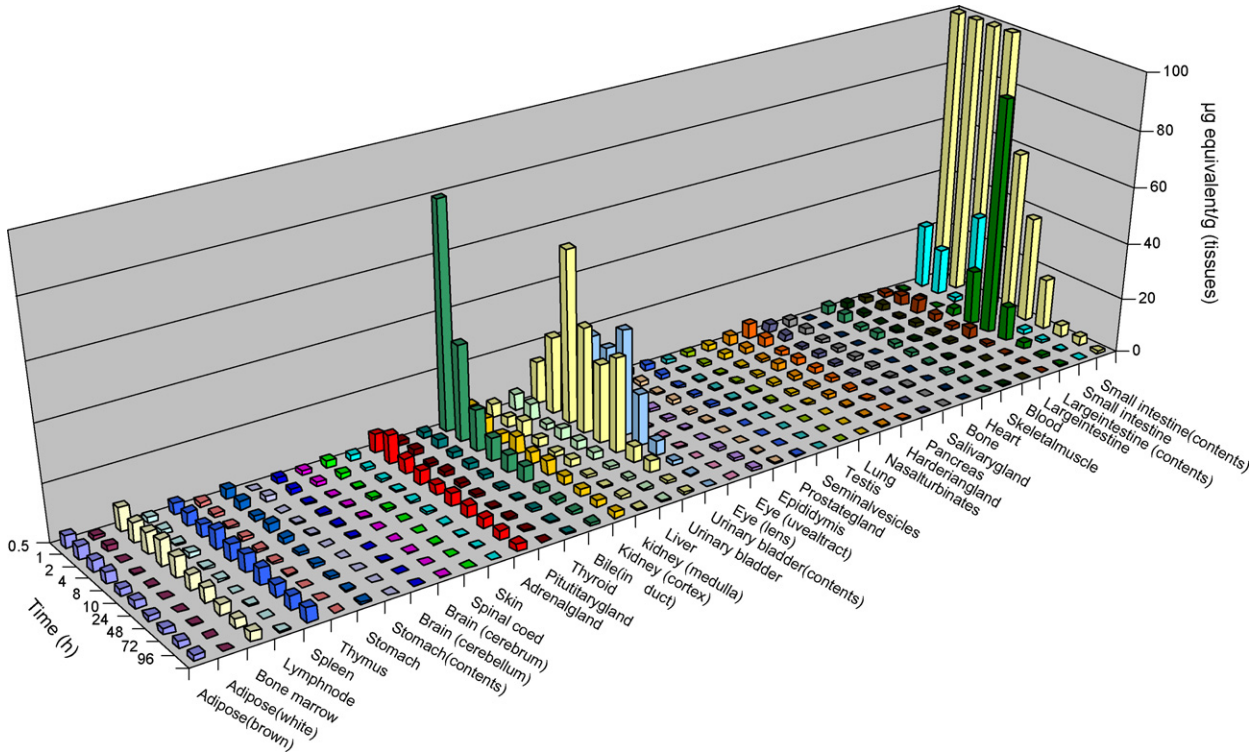

Fig. 4. Mean distribution profile of total radioactivity (μg equivalents/g tissue) of radiolabeled artesunate (AS) in various tissues (column) at 0.5, 1, 2, 4, 8, 10, 24, 48, 72, and 96 h by QWBA technique (top) and at 1, 6, 24, 48, 72, 96, and 192 h by LSC method at single dose of 5 mg/138 μCi/kg to QWBA animals and 5 mg/20 μCi/kg to LSC rats following single intravenous injection of [^{14}C] AS in rats. After i.v. injection the most of radioactivity was distributed in intestines, urinary bladder, bile duct, small and large intestinal contents. The long-lasting and high distribution of [^{14}C] AS were found in spleen, bone marrow, adrenal gland, and adipose in brown partial.

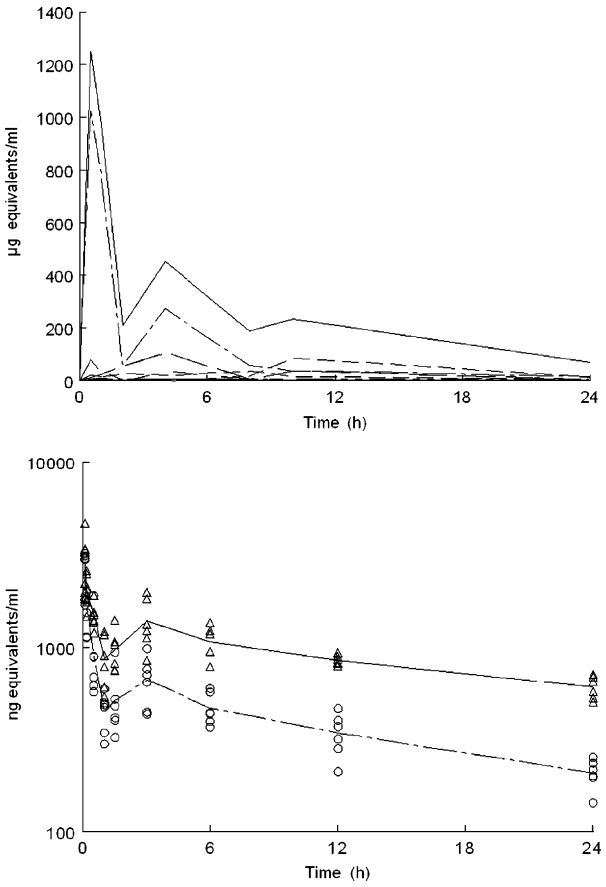

Fig. 5. Multiple concentration peaks of total radioactivity (µg equivalents/g tissue) in total amounts (solid-line) and individual organ and tissue (dashed-line) detected by using quantitative whole-body autography (QWBA, top), and multiple concentration peaks of total radioactivity (ng equivalents/ml) in whole blood (solid-line with triangle markers) and plasma (dashed-line with circle markers) measured by using liquid scintillation counting (LSC) method (bottom), and following a single intravenous injection [^{14}C] artesunate at 5 mg/138 µCi/kg for QWBA and 5 mg/20 µCi/kg for LSC in rats (n = 3–6).

of [^{14}C] AS two peaks of radioactivity were detected (Fig. 5, bottom).

From the ratios between plasma and tissue concentrations it can be estimated how long it takes at minimum to reach equilibrium between tissue and plasma concentration in each organ, where for $K_{t:p}$ values different from one the tissue specific apparent volume of distribution has to be taken into account instead of the real volume [16]. Using the values for AUC ratios from various tissues to plasma reported in Table 1 this estimate reveals that the [^{14}C] AS in all tissue was higher than that in plasma and very higher in several organs, such as spleen, kidneys, adrenal gland and liver (Table 1), suggesting an acidic property of artesunic acid in the tissue distribution [17].

3.4. Equivalence analysis

The mean values of the concentrations were compared separately for PK parameters of C_{max} and AUC_{96h} data in 16 main tissues and organs by using QWBA and LSC methods. The data of radioactivity concentration values and differences, following single [^{14}C] AS intravenous injection, as determined by the QWBA and LSC methods, are shown in Table 1 for individual tissues and organs. In the C_{max} and AUC_{96h} comparison 81% of the major tissues and organs (blood, brain, adrenal gland, muscle, heart, spleen, kidneys, liver, stomach content, large intestine plus content, and small intestine plus content) showed concentration differences on the 90% confidence interval (CI) are within the predefined equivalence range of −20/25% in accordance with US FDA guidance on bioequivalence studies [18,19]. The PK concentrations of [^{14}C] AS measured by QWBA and LSC methods were also very similar (Fig. 3). The only exceptions, not fulfilled within the −20/25% range, were found in the eyes, lungs, and stomach.

The half-lives of the main tissues via LSC evaluation were also similar to those determined by QWBA analysis; however, radioactivity in various tissues was displayed at different time profiles. The longest half-life (slowest disposition) of radiation was found in the spleen and bone marrow at 140–222 h, followed by the lungs (105–123 h), adrenal gland (97–110 h), heart (91–109 h), muscle tissue (96–106 h), kidneys (94–102 h), and blood (82–99 h). In contrast, the radioactivity found in the contents of and in the small intestine and the large intestine had short half-lives of 28–75 h. However, during the treatment period the highest concentration of radioactivity determined by using the LSC assay was found in the tissue of the small intestinal contents, spleen, large intestinal contents, and kidneys. This conclusion is similar to the one obtained through the QWBA analysis (Table 1) which suggests that the two methods provide similar tissue distribution shapes and PK profiles of [^{14}C] AS.

3.5. Multiple concentration peaks and enterohepatic circulation

The multiple concentration peaks of radiolabeled AS, along with a third, were detected in various tissues and organs using QWBA evaluation (Fig. 5, top). Two concentration peaks of [^{14}C] AS were detected in whole blood and plasma using LSC measurements (Fig. 5, bottom). Therefore, the both methods determined the multiple concentration peaks: the first peak formed at 0–0.5 h, the second at 3–4 h, and the third at 8 h after i.v. injection.

4. Discussion

Ever since the phosphor storage imaging plate, together with its scanner, became available 10 years ago, QWBA has been used as a possible substitute for conventional tissue distribution studies. Current experience shows that the accuracy of the QWBA method can be compared to the accuracy achieved by LSC of the tissue samples. The advantages of using the QWBA method are clear. First of all, the anatomical localization of the (non-volatile) radioactivity in freeze-dried whole-body sections minimizes possible diffusion artefacts. In addition, the contamination of parenchyma by body fluid is also avoided, thus avoiding a major problem encountered during tissue dissection procedures. As a result, the concentration of [^{14}C] AS by QWBA method was quantified, by a measure of radioactivity, in more than 40 organs/tissues: a finding two times greater than determined by the LSC assay. The greatest differences in concentrations of radioactivity in organs, determined using the two methods, occurred in the bone marrow, bile (in duct), and various gland organs which were difficult to dissect and measure by LSC method (Table 2).

The biliary metabolic pathway for AS was determined in a present study because 90% of total radioactivity detected was found in the bile and intestinal contents at 0.5 h after i.v. injection by the QWBA method. During the 96 h experimental period, up to 50% of total radioactivity was presented in the small and large intestines, their contents and bile (in duct) following a single intravenous injection of [^{14}C] AS, suggesting that an pathway of the biliary metabolism of AS in rats. Thus the presence of high radioactivity levels in bile is important since it confirms the biliary excretion of AS. However, when using the LSC technique in this study, high lev-

Table 2
Comparison of QWBA (5 mg/138 μCi/kg) and LSC (5 mg/20 μCi/kg) in tissue distribution and metabolic profile findings following a single intravenous dose of [^{14}C] artesunate in male SD rats

Observation findings	QWBA	LSC
Presentation of long-lasting (96–192 h) radioactivity in blood and tissues	Yes	Yes
Alike tissue distribution shape	Yes	Yes
Similar PK assessment of [^{14}C] AS in blood and each tissue	Yes	Yes
Confirmation of the biliary metabolic pathway	Yes	Yes
Determination of multiple level peaks of [^{14}C] AS in blood and tissues	Yes	Yes
Verification of the enterohepatic circulation	Yes	Yes
Full PK evaluation in blood	Yes[a]	Yes[a]
Organs and tissues have been measured and quantified	40	19
Bile (in duct) measurement	Yes	No
Bone marrow and various gland tissues measurements	Yes	No
Tissue/plasma partition coefficients ($K_{t:p}$)	No	Yes
Full PK evaluation in plasma	No	Yes
PK analysis of unchanged AS and DHA in plasma	No	Yes
Determination of AS is the prodrug of DHA	No	Yes
Assessment mass-balance of [^{14}C] AS	No	Yes
Elimination PK analysis of [^{14}C] AS in urine and faeces	No	Yes
Complete hydrolysis pathway of AS to DHA	No	Yes
Conjugation pathway of [^{14}C] AS in plasma, urine, and faeces	No	Yes
Conjugation pathway of unchanged AS and DHA in plasma	No	Yes
Drug distribution in plasma and red blood cells	No	Yes
Drug protein binding with whole blood and plasma	No	Yes
Metabolites identification in plasma free and conjugation fractions	No	Yes
Metabolites identification in urine and faeces	No	Yes

[a] The PK analysis of [^{14}C] AS by using QWBA method with data of 10 time points, whereas using LSC method with 14 time points (n = 3–5).

els of radioactivity were found only in the small intestinal contents without bile data. The QWBA method on the other hand replenished the shortage of the LSC method by finding high levels of radioactivity in the bile. Additionally, determining the concentration of radioactivity in the bone marrow is extremely difficult using the LSC method but the QWBA technique can accurately determine the radioactivity present. For example, the QWBA evaluation demonstrated that the half-life of radioactivity in the bone marrow was 153 h and the radiolabel was 12% of total [^{14}C] AS. The high concentration and long half-life of [^{14}C] AS (metabolites) in bone marrow may relate to the reversible anemia, reticulocytopenia and hemotoxicity, which were previously reported in animals and humans [20–25].

In this study, multiple concentration peaks and biliary excretion concentrations were demonstrated using two methods (QWBA and LSC). The results indicated that 0.5–1 h after dosing, most of the [^{14}C] AS was extracted into the liver after which it was excreted into the intestines via bile ductules. The increase of the radioactivity of AS in other tissues, after 3–4 h, can be attributed to the re-absorption of the drug after it had left the intestines. The deposition of artemisinin drugs was mostly by biliary excretion and intestinal re-absorption [11]. Furthermore, [^{14}C] AS's (metabolites) lengthy presence (192 h) in the rat, can most likely be attributed to the continuous re-absorption and enterohepatic cycling. Recently, we found that a less polar metabolite of AS is about 42–65% of chromatograph in both free and conjugation fractions at 24 h after incubation with human and rat hepatocytes (our unpublished data). This one may relate to the long-lasting metabolite(s), and further identification study is going on.

The multiple radioactivity peaks shown in the plasma, blood and various tissues indicate the presence of enterohepatic circulation of [^{14}C] AS in all subjects. The drug plasma concentration profile revealed that [^{14}C] AS formed a secondary and third peak at 3–4 and 7–8 h after i.v. injection (Fig. 5). This again suggests that the multiple increases in drug concentration are due to either enterohepatic circulation or the presence of a multiple absorption phases [26–28]. Usually, multiple peaks in oral concentration–time profiles, following drug administration, are a result of: (1) discontinuous absorption along the gastrointestinal tract, (2) post-absorptive storage and release, (3) and/or enterohepatic circulation [29]. In these cases, the multiple peaks seen and the concentrations of radioactivity in biliary excretions determined after the i.v. injection of AS strongly suggest the presence of an enterohepatic circulation [30–33].

Partitioning into the different tissues largely determines the fate of a xenobiotic after it is introduced into the body. Thus, knowledge about the extent of this partitioning is of great importance for an understanding of a compounds pharmacokinetics and the assessment of its toxicological or pharmacological potential. Particularly for the application of physiology based pharmacokinetic modelling in such an assessment, knowledge of the steady state tissue/plasma partition coefficients ($K_{t:p}$) for all organs explicitly contained in the model is indispensable, since they represent a large part of the most important compound specific model parameters. The methodology presented here is a generally applicable and straightforward approach to calculate tissue/plasma partition coefficients [16] by LSC method with radiolabeled AS. Its use allows an easy estimate of tissue exposition for all kinds of organic substances based on a few physicochemical properties and the unbound fraction in plasma [34]. The present approach is based on mechanistic principles that are very similar to those underlying previous methods for calculating tissue/plasma partition coefficients [16]. It cannot be excluded than in some cases the uptake into tissue is additionally limited by a membrane permeation process. This is particularly true for the brain where the blood–brain barrier is known to control the uptake kinetics in many cases. Thus it is not surprising that the high partition coefficients of the acidic AS are observed in brain (2.42), RBC (3.51), and very high that in spleen (63.22) and kidneys (28.25) [34].

5. Conclusion

Present studies propose satisfactory comparisons between the two techniques, indicating that the accuracy of the quantification of the imaging plates can be similar to the accuracy of liquid scintillation of tissue dissection. Even though the QWBA method has some advantages in quantitative determination of radioactivity present in all organs and many small substructures, especially in bile (in duct) and bone marrow tissues as shown by the present study, the LSC technique still determines greater distribution profiles and more metabolic messages than that by QWBA such as (i) the full PK evaluation of radiolabeled AS was conveyed in blood and plasma; (ii) the full PK analysis of unchanged AS and DHA was reported in plasma; (iii) tissue/plasma partition coefficients; (iv) the complete hydrolysis pathway of AS to DHA; (v) the mass-balance of [^{14}C] AS was assessed from rat urinary and faecal excretions; (vi) the elimination rates detailed in urine and faeces; (vii) the conjugation pathway of radiolabeled AS was found in plasma, urine and faeces; (viii) the conjugation metabolism of unchanged AS and DHA was located in plasma and urine; (ix) the radiolabeled AS was distributed in plasma and red blood cells; (x) [^{14}C] AS bonded, through protein binding, with whole blood and plasma; (xi) the metabolites of AS were identified [11] (Table 2). Therefore, the two methods can provide us a more detail

and comprehensive evaluations on the tissue distribution and metabolic profiles of [^{14}C] AS after intravenous injection.

Acknowledgements and financial support

This study was supported by the United States Army Research and Materiel Command. The opinions or assertions contained herein are the private views of the author and are not to be construed as official, or as reflecting true views of the Department of the Army or the Department of Defense.

References

[1] S. Ullberg, Acta Radiol. Suppl. 118 (1954) 1–110.
[2] N. Motoji, E. Hayama, A. Shigematsu, Eur. J. Drug Metab. Pharmacokinet. 20 (1995) 89–105.
[3] L. van Beijsterveldt, R. Geerts, T. Verhaeghe, B. Willems, W. Bode, K. Lavrijsen, W. Meuldermans, Arzneim-Forsch/Drug Res. 54 (2004) 85–94.
[4] K. Inazawa, M. Koike, T. Yamaguchi, Exp. Mol. Pathol. 76 (2004) 153–165.
[5] S. Jacob, A.E. Ahmed, Pharmcol. Res. 48 (2003) 479–488.
[6] K. Kai, H. Satoh, T. Kajimura, M. Kato, K. Uchida, R. Yamaguchi, S. Tateyama, K. Furuhama, Toxicol. Pathol. 32 (2004) 701–709.
[7] E.G. Solon, F. Lee, J. Pharmcol. Toxicol. Methods 46 (2002) 83–91.
[8] U. Busch, G. Heinzel, G. Nehmiz, Regul. Toxicol. Pharmacol. 31 (2000) S45–S50.
[9] R. d'Argy, A. Sundwallx, Regul. Toxicol. Pharmacol. 31 (2000) S57–S62.
[10] W. Steinke, Y. Archimbaut, M. Becka, R. Binder, U. Busch, P. Dupont, J. Maas, Regul. Toxicol. Pharmacol. 31 (2000) S33–S43.
[11] Q. Li, L.H. Xie, A. Haeberle, J. Zhang, J.P.J. Weina, Am. J. Trop. Med. Hyg. 75 (2006) 817–826.
[12] M.J. Potchoiba, M. West, M.R. Nocerini, Drug Metab. Dispos. 26 (1998) 272–277.
[13] A. Schweitzer, A. Fahr, W. Niederberger, Int. J. Rad. Appl. Instrum. [A] 38 (1987) 329–333.
[14] E.G. Solon, L. Kraus, J. Pharmacol. Toxicol. Methods 46 (2001) 73–81.
[15] Q. Li, L.H. Xie, Y.Z. Si, E. Wong, R. Upadhyay, D. Yanez, P.J. Weina, Int. J. Toxicol. 24 (2005) 241–250.
[16] W. Schmitt, Toxicol. In Vitro. 22 (2008) 457–467.
[17] T. Rodgers, M. Rowland, J. Pharm. Sci. 95 (2006) 1238–1257.
[18] FDA Guidance for Industry, 2001, http://www.fda.gov/cder/guidance/3616fnl.htm.
[19] FDA Guidance for Industry, 2003, http://www.fda.gov/CDER/guidance/5356fnl.pdf.
[20] X.T. Cao, D.B. Bethell, T.P. Pham, T.T. Ta, T.N. Tran, T.T. Nguyen, T.T. Pham, T.T. Nguyen, N.P. Day, Trans. R. Soc. Trop. Med. Hyg. 91 (1997) 335–342.
[21] I. Itoda, T. Yasunami, K. Kikuchi, H. Yamaura, K. Totsuka, K. Yoshinaga, M. Teramura, H. Mizoguchi, T. Hatabu, S. Kano, Kansenshogaku. Zasshi. 76 (2002) 600–603.
[22] I.R. Ribeiro, P. Olliaro, Med. Trop. (Mars). 58 (1998) 50–53.
[23] A. Same-Ekobo, J. Lohoue, E. Essono, L. Ravinet, Med. Trop. (Mars). 59 (1999) 43–45.
[24] S. Yoshizawa, K. Hike, K. Kimura, T. Matsumoto, N. Furuya, K. Tateda, S. Kano, K. Yamaguchi, Kansenshogaku. Zasshi. 76 (2002) 888–892.
[25] L.H. Xie, T.O. Johnson, P.J. Weina, Y.Z. Si, A.S. Haeberte, R. Upadhyay, E. Wong, Q.G. Li, Int. J. Toxicol. 24 (2005) 251–264.
[26] A. Lindholm, S. Henricsson, R. Dahlqvist, Br. J. Clin. Pharmacol. 29 (1990) 541–548.
[27] Y. Matsuzawa, T. Nakase, J. Pharmacobio-dyn. 7 (1984) 776–783.
[28] D. Westerling, L. Frigren, P. Hoglund, Ther. Drug Monit. 15 (1993) 364–374.
[29] A.B. Suttle, K.L. Brouwer, Drug Metab. Dispos. 22 (1994) 224–232.
[30] D. Brewster, M.J. Humphrey, M.A. McLeavy, Xenobiotica 11 (1981) 189–196.
[31] T. Ogiso, T. Kitagawa, M. Iwaki, T. Tanino, Biol. Pharm. Bull. 20 (1997) 405–410.
[32] A. Scharl, M.W. Beckmann, J.E. Artwohl, S. Kullander, J.A. Holt, Int. J. Radiat. Oncol. Biol. Phys. 21 (1991) 1235–1240.
[33] T.J. Visser, M. Rutgers, W.W. de Herder, S.J. Rooda, M.P. Hazenberg, Acta Med. Austriaca 15 (1988) 37–39.
[34] T. Rodgers, M. Rowland, J. Pharm. Sci. 95 (2006) 1238–1257 (erratum in: J. Pharm. Sci. 96 (2007) 3153–3154).